Construction and Building Materials 181 (2018) 447–454

Contents lists available at ScienceDirect

Construction and Building Materials

journal homepage: www.elsevier.com/locate/conbuildmat

Correlation between destructive compression tests and non-destructive ultrasonic measurements on early age 3D printed concrete

R.J.M. Wolfs *, F.P. Bos, T.A.M. Salet

Department of the Built Environment, Eindhoven University of Technology, Eindhoven, The Netherlands

HIGHLIGHTS

- Non-destructive ultrasonic tests were performed on early age 3D printed concrete.
- Results of the ultrasonic tests were compared with uniaxial compression tests.
- A linear correlation was found between pulse velocity, strength, and stiffness.
- The study stimulates development of online ultrasonic methods for 3D printing.

ARTICLE INFO

Article history:
Received 12 April 2018
Received in revised form 6 June 2018
Accepted 7 June 2018

Keywords:
3D Printing
Fresh concrete
Mechanical properties
Compression test
Ultrasonic testing

ABSTRACT

3D printing of concrete and related digital fabrication techniques are enjoying rapid growth. For these technologies to be broadly accepted in structural applications and to be economically competitive, quality control methods of the process will be required. Additive concrete manufacturing processes are sensitive to process settings and conditions, which calls not only for preprint structural modelling to establish printability, but also for in-print monitoring to ensure expected properties are indeed achieved. Non-destructive test methods are highly suitable for this aspect of quality control, as they usually allow efficient, high frequent digital measurements that require relatively little effort. However, as they generally do not directly measure the appropriate parameter(s), correlations between non-destructive and destructive testing have to be established. The preprint structural modelling is based on a number of time-dependent mechanical properties, including the compressive strength and the Young's modulus. If concrete is still in the dormant state, as it often is in 3D concrete printing, these properties require difficult, time consuming destructive tests to establish. In the present work, the correlation between these two mechanical properties on the one hand, and the pulse velocity on the other, was studied. A (destructive) unconfined uniaxial compression test was applied to determine the former, while a (non-destructive) ultrasonic wave transmission test was used for the latter. As expected from previous research on a similar mortar, both the compressive strength and the Young's modulus were found to increase linearly in a time frame of 5–90 min after extrusion. This is attributed to thixotropic build-up. Within that time frame, the pulse velocity also grew in a linear fashion. Thus, a simple linear correlation between the destructive and non-destructive test results could be established. For now, this allows continuous quality control on simply obtainable control batches. Furthermore, it stimulates the development of ultrasonic online monitoring methods for the objects during printing.

1. Introduction

Presently, a rapidly growing number of innovative case-study structures is being presented that have been realized through various forms of additive manufacturing methods of concrete and cementitious materials. It is increasingly recognized by industry and clients that these technologies present a serious potential in terms of optimized material use, reduced labour, and form freedom. The focus, by and large, is on delivering proofs of concept which show the aesthetical and economical potential. In most cases, extrusion-type methods with a nozzle attached to various types of moving robots are applied [1–5]. These layer-wise extrusion processes are commonly referred to as (3D) concrete printing.

* Corresponding author.
E-mail address: r.j.m.wolfs@tue.nl (R.J.M. Wolfs).

https://doi.org/10.1016/j.conbuildmat.2018.06.060
0950-0618/

Some associated technologies are simultaneously under development, such as D-Shape (based on binder jetting) [6], Mesh Mould [7], and Smart Dynamic Casting [8,9]. Digitally Fabricated Concrete (DFC) is used as a generic term to refer to these innovations. Their common denominator is the perspective to move towards largely automated production. The study presented in this paper relates to 3D Concrete Printing (3DCP) technology under development at the Eindhoven University of Technology [10].

Owing to the novelty of concrete printing, the structural properties of the fabricated object, both during and after printing, are often only globally understood. Significant knowledge gaps still exists concerning the specific relations between the design, material, system, and product. It is known from other 3D printing industries, these parameters interact heavily and significantly influence the quality of the fabricated product [11]. Structural collapse during printing and layer delamination afterwards are common failures associated with insufficiently attuned processes. To avoid such failures to occur, and to prove that the manufactured object is equal to the design, quality control procedures should be introduced to DFC. As such, the authors suggest a development towards a system in which:

(1) the manufacturing process is monitored continuously,
(2) the acquired data is used for real-time quality control, and
(3) a closed feedback loop reacts upon the quality control when required.

Primarily, this concerns a measuring method in line with the digital nature of the manufacturing process. In conventional concrete construction, type testing (e.g. cube compression tests, slump-flow tests) is a commonly applied instrument to prove certification compliance and thus to show sufficient quality has been obtained. However, the continuous nature of the printing process and the presence of interacting parameters, make such isolated and destructive tests unsuitable. Instead, an online non-destructive monitoring system is required, which can measure properties on every position and moment in the process.

To assess the quality, or structural integrity, of the printed object based on the online measurements, initial steps towards the structural analytical and numerical modelling of the 3DCP process have been presented [12,13]. These modelling methods aim to predict the structural performance and possible failure modes of objects during printing, based on mechanical properties as defined by the printing process. Further development of modelling methods will be required to predict other crucial properties, such as the interface adhesion, which depends on interval time and application pressure among others.

Likewise, early examples of online monitoring and feedback systems were introduced. Lloret et al. adopted a method of simultaneous penetrometer tests during extrusion to record the concrete strength evolution [8], and formwork pressure and friction measurements [9], to adjust the robot speed accordingly. Neudecker et al. [14] proposed a feedback loop for robotic spraying of concrete, where 3D scanners measure the surface finish of the sprayed concrete parts. Wolfs et al. [15] presented a continuous measurement and real-time adjustment of print height nozzle relative to the print surface (or previous layer) for the 3DCP system.

This study takes a first step in connecting the structural modelling on 3DCP objects during printing as introduced by the authors [12] with continuous monitoring of the mechanical properties that are used in such modelling. In particular, the correlation of parameters from a non-destructive test method with potential for online monitoring, to mechanical properties determined from an appropriate destructive test for concrete in the dormant state is established.

2. Theoretical framework

2.1. Concrete hydration and the 3DCP process

Concrete goes through several stages during 3D printing that can be organized by its hydration processes and relative to the printing process. The four stages of hydration are: (1) the initial hydration directly after mixing, when the cement first comes in contact with water, (2) the dormant stage in which the cementing reactions are delayed, and the mechanical properties are mainly determined by thixotropic build-up attributed to both interparticle forces and low-rate hydration reactions [16], (3) the setting stage when cementing reactions accelerate and the materials hardens, (4) the hardened stage when the cementing reactions decelerate. On the other hand, 3 stages can be distinguished relative to the print process: (1) pre-deposition, when the concrete is still in the print system, (2) post-deposition/in-print, when the concrete is being printed, (3) after printing, when the print process is finished. The hydration and print process stages do not necessarily develop in parallel, rather the extent of that alignment depends heavily on the particular print material, print system and object design. Moreover, competing requirements may be found in the required performance in each stage.

The pre-deposition stage concerns the material in a fluid, moving state, while being transported through a system of pump, hose and nozzle. In this phase, a high workability is desirable to minimize friction, prevent blockage or fracture in the system and guarantee extrusion of the desired cross section [17–19]. Furthermore, considering recent developments in the field of (fibre) reinforcement of 3D printed concrete [20,21], the material should be fluid enough to compact around such reinforcement and realize proper bond.

The in-print stage concerns the material in an intermediate and static state. Here, the extruded concrete should be shape-stable with a sufficient strength and stiffness development to sustain the subsequent deposited layers and guarantee stability of the printed geometry [17,22,23]. Generally, the strength and stiffness in the dormant phase fulfils this requirement up to a certain object height, after which the setting stage should initiate to maintain the desired building rate.

Finally, the concrete is in a solid, hardened state, where sufficient bond strength between the layers is required. If the hydration process during printing is too quick, or the printing speed too low, the layers may not longer bond properly, resulting in poor structural integrity of the printed product [24–26]. Thus, understanding the transition between stages and the properties of concrete within each stage is critical to guarantee a robust printing process and a structurally safe end product.

2.2. Monitoring mechanical properties of early age concrete

A typical print duration in 3DCP is several minutes up to two hours. With the print materials that are currently being used in the process, the critical stage during printing is when the concrete is in the dormant stage. As the structural integrity during printing can be predicted through analytical and numerical modelling that have shown it to be highly sensitive to the early age mechanical properties, monitoring these properties is of particular interest for quality control. Due to thixotropic build-up in static conditions, they are time-dependent and develop significantly within the time-span of a typical printing process (as has been shown by the authors [12]), but are also expected to rely on a number of other variables in the print process that are difficult to predict or control (e.g. induced energy through pumping and system friction, compaction/density, temperature).

This requires a measuring method that is easy to perform and provides a continuous or high frequent measurement output. Often, empirical tests are applied, e.g. Vicat or penetrometer tests [27]. Although a correlation with compressive strength or yield stress may exist [28], such tests are often not continuous, susceptible for manual influence, and of a destructive nature. Considering the digital workflow of 3D printing and aiming at a high-quality manufacturing method, non-destructive testing (NDT) methods are preferred. The use of NDT has already been adopted in other 3D printing industries. Post-process inspection methods based on e.g. liquid penetration or thermography can be used for quality control of the end product. Moreover, visual and ultrasonic methods can also be applied during 3D printing to inspect the properties and process as the object is being constructed [29].

Ultrasonic measurement methods are of particular interest for 3D concrete printing, as they have already been adopted in the construction industry to monitor the material development of (fresh) concrete in a continuous, non-destructive way. These methods measure the transmission or reflection velocity of sound waves through a sample at a high frequency. Ultrasonic methods are applied in concrete manufacturing and construction, for instance to estimate the strength development of cast concrete so that the demoulding sequence can be optimized [30], as well as to monitor extrusion-based slip-form manufacturing [31].

2.3. Ultrasonic pulse velocity test

To be able to use the measured ultrasonic velocity to determine mechanical properties that can also be directly derived from destructive testing, a correlation between the targeted parameter (s) and the measured parameter has to be established.

Generally, the pulse velocity increases as the amount of hydration products grows, which also holds for the mechanical properties. However, their rate of development is not necessarily equal. It was reported by Voigt et al. [32] that certain early hydration products create a structure which contribute positively to the propagation of sound waves, but not significantly to the strength and stiffening behaviour. Moreover, the ultrasound measurements are dependent on: cement type, aggregates, and presence and dosage of admixtures like accelerators and superplasticizers [33,34].

Notwithstanding these dependencies, correlations between ultrasonic pulse velocity and mechanical properties have been established, for instance by [32,34–38]. However, they are generally applied for stages when the concrete has an age of at least several hours. Since concrete is in a principally different stage of development during 3D printing, governed by thixotropy rather than setting or hardening processes, these relations are not necessarily applicable. Therefore, this study aims to determine a correlation between (i) ultrasonic pulse velocity and Young's modulus, and (ii) ultrasonic pulse velocity and compressive strength in a time frame of 5–90 min after extrusion, for the applied print mortar. Because a correlation between compressive strength and shear strength development in the dormant stage has already been established by the authors [12], these correlations between pulse velocity, Young's modulus and compressive strength suffice to check the actual structural development of the material to that on which a numerical model could be based.

3. Experimental program

3.1. Material and 3D printing system

In this research, a custom designed printable mortar *Weber 3D 145-1* was applied, containing Portland cement (CEM I 52.5 R), siliceous aggregate with a maximum particle size of 3 mm, limestone filler, additives, rheology modifiers and a small amount of polypropylene (PP) fibres. This is an improved version of the mortar introduced by Bos et al. [10] that has since been branded *Weber 3D 115-1*. The fresh concrete is extracted after mixing and pumping using the 3DCP setup [10], which consists of an M-Tec DuoMix 2000 mixer-pump with a linear displacement pump that feeds concrete through a Ø25 mm, 10 m length hose (Fig. 1). Consistent mixing speed and pumping frequency are maintained for every test. All experiments were conducted at room temperature $T = 21$ °C.

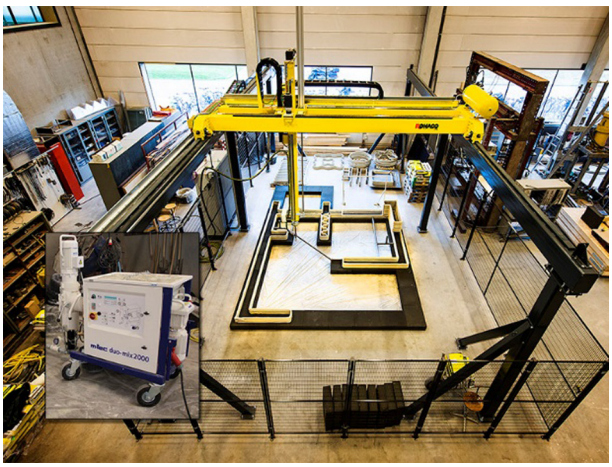

Fig. 1. 3DCP setup, consisting of 4 axis gantry robot, numerical control unit, and concrete mixer and pump.

3.2. Uniaxial unconfined compression test

Two time-dependent mechanical properties, the Young's modulus E(t) and the compressive strength $f_c(t)$, were directly determined from an Unconfined Uniaxial Compression Test (UUCT), custom developed to early age 3D printed concrete. The details and background to this test have been extensively described in [12]. Some aspects that are crucial to the interpretation of the results, are repeated here.

The compression tests were carried out to determine the mechanical properties at distinct concrete ages of $t = 5$, 15, 30, 60 and 90 min. Here $t = 0$ is defined as the time of compaction directly after extrusion, i.e. the moment when the concrete is no longer in motion, approximately 2 min after water and cement first come into contact in the mixer-pump. The time range up to 90 min corresponds to the typical duration of a 3D printing process.

The early age strength and stiffness properties were derived by UUCT on cylindrical concrete samples. The specimen dimensions were designed according to ASTM D2166 [39]. A cylinder diameter of d = 70 mm and height of h = 140 mm were chosen to eliminate particle size effect, and to allow a diagonal shear failure plane to form. The fresh concrete was extracted into steel cylindrical moulds lined with a thin sheet of Teflon and compacted for 5 s on a 30 Hz vibration table to realize a homogeneous sample. Just before testing the sample was carefully demoulded and the Teflon sheet removed.

The samples were loaded in an INSTRON test rig equipped with a 5 kN load cell and two stiff cylindrical loading plates with a diameter equal to the specimens. The tests were performed displacement controlled at a rate of 30 mm/min, chosen to mimic the loading rate during printing. In total 5 specimens were tested for each concrete age, resulting in a total of 25 UUCT specimens.

During the test, the compressive force, and the vertical and lateral deformation were recorded. The deformations were recorded by image analysis. High resolution (18 MP) photographs were taken during testing, which were post-processed in National Instruments Vision Builder software.

3.3. Ultrasonic wave transmission test

Simultaneously, a non-destructive ultrasonic wave transmission test (UWTT) was used to continuously monitor the velocity of sound through a printed sample in a time span of 5–90 min.

The ultrasonic wave transmission test were performed using compression (P) waves according to NEN-EN 12504-4 [40]. A commercial available system was used (type IP8, manufactured by UltraTest GmbH, Germany). The UWTT system (Fig. 2) consists of a cylindrical concrete sample with diameter $d = 50$ mm and height $h = 50$ mm, cast into a silicon mould with high damping properties. On two sides of the sample a transmitter and receiver are placed with a mutual distance of 40 mm. Four sound absorbers are positioned in the silicon mould to avoid influences of waves travelling through the mould, bypassing the sample. An ultrasonic pulse is transmitted every 1 min over a period of at least 90 min. The propagation time t of the pulse over the wave path l is recorded and used to compute the P-wave

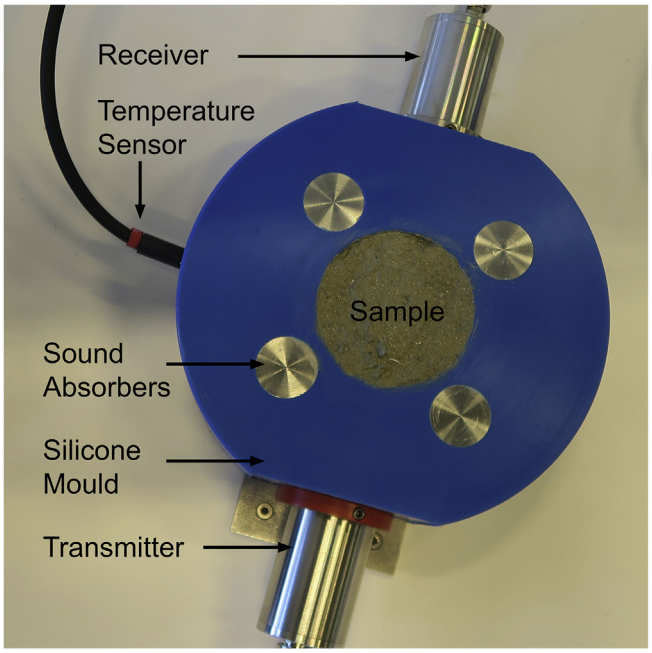

Fig. 2. Ultrasonic wave transmission equipment.

velocity $v = l/t$ through the fresh material. Subsequently, the acceleration v' was calculated as the first derivate of the P-wave velocity function. Additionally, the sample temperature was measured continuously during each test.

For each series of uniaxial tests (t = 5–90 min) one parallel ultrasonic test was performed using the same material batch as extracted from the 3DCP setup, resulting in a total of 5 UWTT specimens. Each UWTT sample was compacted by tapping three times with a rod to realize a homogeneous sample.

4. Results

4.1. Uniaxial unconfined compression

The cylindrical samples were loaded in compression up to 30% strain. Typical load-displacement curves are shown in Fig. 3 for concrete age t = 30 min, were the five grey lines represent each individual test, and the black line indicates their average. Each load-displacement curve was then translated into a stress-strain relation, taking into account large deformations of the samples. The updated cross section, derived by image analysis, was used to calculate the actual state of stress during the tests. Fig. 4 shows

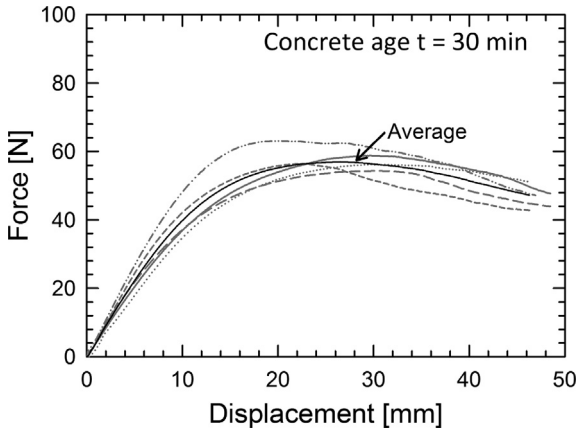

Fig. 3. Force-displacement diagram of compression test for concrete age t = 30 min.

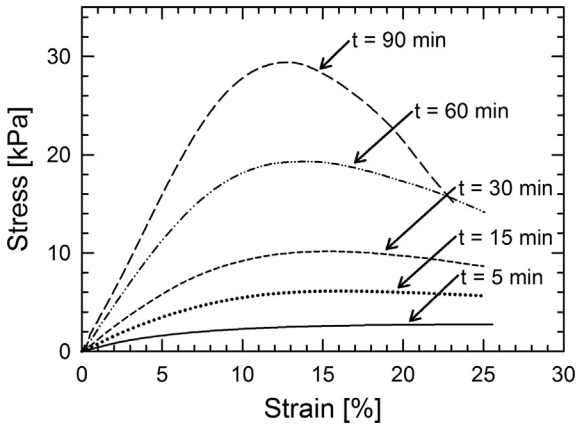

Fig. 4. Average stress–strain relations for each concrete age t = 5–90 min.

the average stress-strain relation for each concrete age, t = 5–90 min. The stress-strain data was cut off at 25% strain, after which the samples were significantly deformed and image analyses provided unrealistic values.

The unconfined compressive strength f_c is defined for each test as the maximum occurring stress after area correction, and is summarized in Table 1 along with each sample's Young's modulus measured at 5% strain, and density. The Poisson's ratio, derived from lateral deformations at 5% strain, appeared to be constant in the first 90 min and was equal to v = 0.3. Typical failure modes for the subsequent specimen sets are shown in Fig. 5.

The early age samples (e.g. t = 5 and 15 min) fail by plastic barrelling, which generally transform into a brittle shear failure plane for specimens of older age (e.g. t = 60 and 90 min). The intermediate samples show a transitional failure behaviour.

In Fig. 6, linear trend lines are presented for both the compressive strength and the elasticity modulus development. For comparison, the results from an earlier study on the previously developed Weber 3D 115-1 mortar are also shown. Based on the results of the compression tests, the compressive strength and Young's modulus for Weber 3D 145-1 can be defined as a function of concrete age, given by Eqs. (1) and (2), respectively:

$$f_c(t) = 0.314 \cdot t + 1.109 \quad (1)$$

$$E(t) = 3.423 \cdot t + 17.369 \quad (2)$$

The rate of development of strength and elasticity modulus is compared in Fig. 7.

4.2. Ultrasonic wave transmission

The ultrasonic pulse velocity was recorded for 5 samples, indicated by the grey lines depicted in Fig. 8-left. The black continuous line represents the average velocity, which can be approximated by a linear fit in the studied time frame. Fig. 8-right gives the measured sample temperatures and wave acceleration. Based on the results of the ultrasonic tests, the ultrasonic pulse velocity can be expressed as a function of concrete age, given by Eq. (3):

$$v_p(t) = 3.851 \cdot t + 66.68 \quad (3)$$

5. Discussion

5.1. UUCT

As expected from previous research, Fig. 4 shows the mechanical properties of the print mortar develop significantly within the

Table 1
Compressive strength, Young's modulus and density derived from the Uniaxial Unconfined Compression Test, with average values μ, standard deviation SD, and relative standard deviation RSD.

Concrete age [min]	Compressive strength f_c [kPa]			Young's modulus E [kPa]			Density ρ [kg/m^3]		
	μ	*SD*	*RSD*	μ	*SD*	*RSD*	μ	*SD*	*RSD*
5	2.777	0.484	17%	35.924665	6.176604	17%	2111.0	8.8	0.4%
15	6.153	0.927	15%	69.3797	8.050724	12%	2191.8	25.1	1.1%
30	10.233	1.477	14%	115.84385	20.10911	17%	2167.2	7.8	0.4%
60	19.350	1.883	10%	225.37703	26.38941	12%	2172.8	11.1	0.5%
90	29.740	4.084	14%	324.85337	54.57381	17%	2229.1	8.0	0.4%

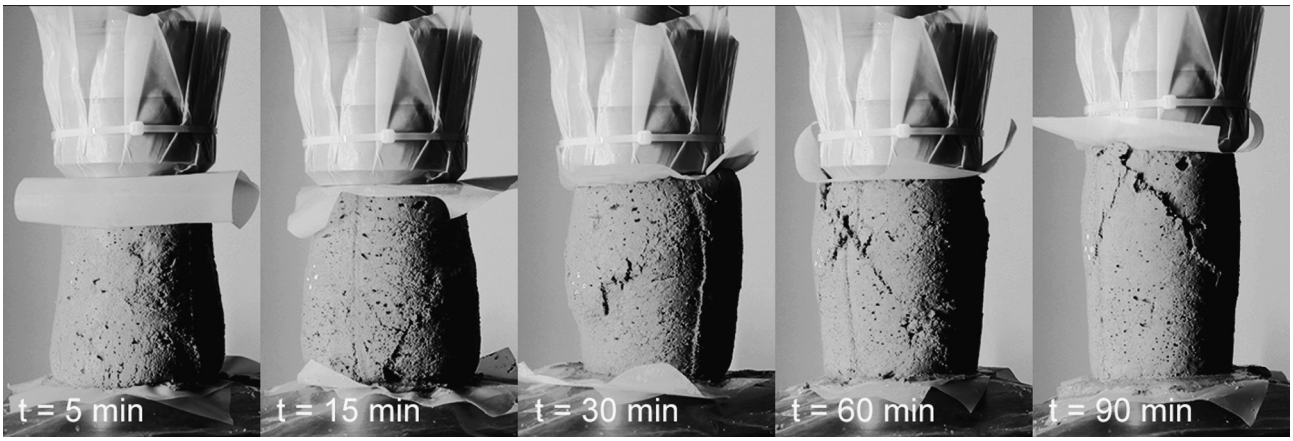

Fig. 5. Failure modes as observed in the compression tests, for concrete age *t* = 5–90 min.

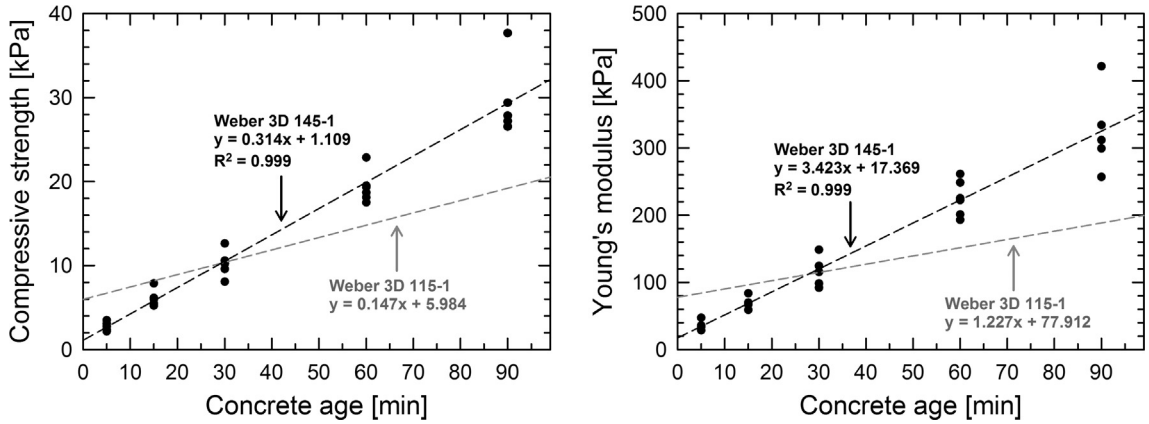

Fig. 6. Compressive strength development (left) and Young's modulus development (right) up to 90 min for Weber 3D-145-1 derived from the compression tests. The black marks indicate the individual test results, and the dashed black line represents a linear fit based on the average test results. For comparison, the dashed grey line represents the results of a previous study on an earlier developed mortar, Weber 3D 115-1.

time frame of a typical printing process. Globally, the mortar behaviour tested in this study (*Weber 3D 145-1*) is very similar to that of the mortar (*Weber 3D 115-1*) investigated in the previous study [12]. Both the strength and Young's modulus increase with concrete age, as can be recognized from the increment of the maximum stress and of the initial slope in the stress-strain relations, respectively. As in the earlier study, the increases are linear over time, and maintain an approximately equal rate, as evidenced by Figs. 6 and 7, respectively. Linear rates of development of fresh concrete before initial setting are also commonly reported in literature, measured both destructively [16,41] and non-destructively [32], although the latter usually refer to concrete older than 2 h, after which the linear trend no longer holds.

The *Weber 3D 145-1* mortar has a lower initiation of early age strength and modulus of elasticity, but a higher rate of development (steeper lines in Fig. 6, initiating from a lower starting point). The lower initial material stiffness is desirable considering a consistent workability throughout the printing process, as it minimizes the internal system friction and material fracture during extrusion. The following, relatively rapid, rate of mechanical properties development is desirable from a buildability perspective, i.e. the consecutive placement of layers and the overall stability of the printed geometry.

In addition, a gradual transition in the failure behaviour can be recognized, from a plastic towards a more brittle behaviour. This is shown both by the changing of the stress-strain curve that develops an increasingly distinct peak at higher ages, and by the failure behaviour illustrated by Fig. 5. A similar failure transition was reported for various experiments on early age concrete by Mettler et al.[42]. A further subdivision in the dormant stage of concrete

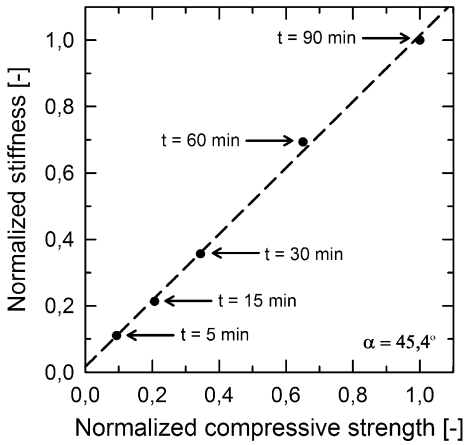

Fig. 7. Comparison between the strength and stiffness development up to 90 min. All values are normalized to their maximum average value at t = 90 min.

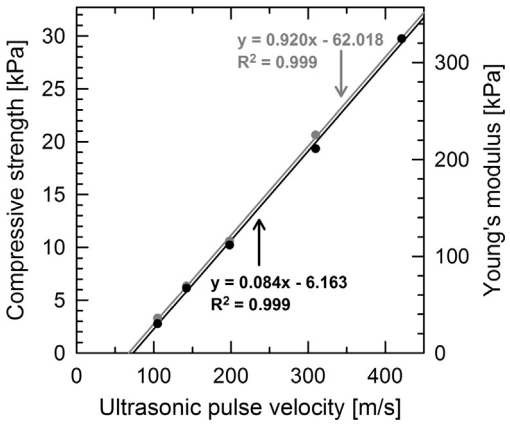

Fig. 9. Ultrasonic pulse velocity versus compressive strength (in black) and Young's modulus (in grey).

development (as discussed in Section 2.1) could be introduced, but this falls outside the scope of the current study.

5.2. UWTT

Both the sample temperature and wave acceleration are mostly constant in the time frame considered (Fig. 8-right). The minor decrease in the first minutes may be attributed to an initial increment of temperature before extrusion due to the accumulated heat in the mixer-pump, and the heat released by initial hydration reactions. After that, the hydration reactions come to a rest and the sample temperature reaches the ambient value. Logically, the constant wave acceleration should result in a linearly increasing pulse velocity, which was indeed found (Fig. 8-left). After 90 min, it has reached a speed of v_p = 400 m/s, well below the v_p value between 1400 and 1500 m/s, that is typically found as indicator of initial setting [43,44]. Therefore, it appears the increment of pulse velocity may be attributed solely to the thixotropic build-up of the material.

5.3. Correlation of UUCT and UWTT parameters

The results of the destructive UUCT and the non-destructive UWTT are compared in Fig. 9. As would be expected from the fact that both show linearly increasing parameters over time, their correlation may be approximated accurately by *linear* trend lines. The relations between the ultrasonic pulse velocity, and both the early age Young's modulus (in grey) and compressive strength (in black) of Weber 3D 145-1, are given by Eqs. (4) and (5), respectively, which are remarkably more simple than the relations presented by for instance [35,38] that apply to concrete beyond the time frame considered here.

$$E(t) = 0.920 v_p(t) - 62.018 \quad (4)$$

$$f_c(t) = 0.084 v_p(t) - 6.163 \quad (5)$$

As the relation between these tests is now established, the results of the non-destructive measurements can be used to assess the structural integrity (or buildability) of 3D printed objects in the fresh material state.

6. Conclusions

The early age mechanical properties which are required for structural analysis of a 3D concrete printing process can be determined directly through destructive tests or indirectly through non-destructive methods that measure associated variables. In this study, the correlation between the compressive strength and the Young's modulus obtained from unconfined uniaxial compressions tests, and the pulse velocity taken from ultrasonic wave transmission tests (all of which are time dependent) in the critical phase for the printing process, i.e. in the dormant material state up to 90 min

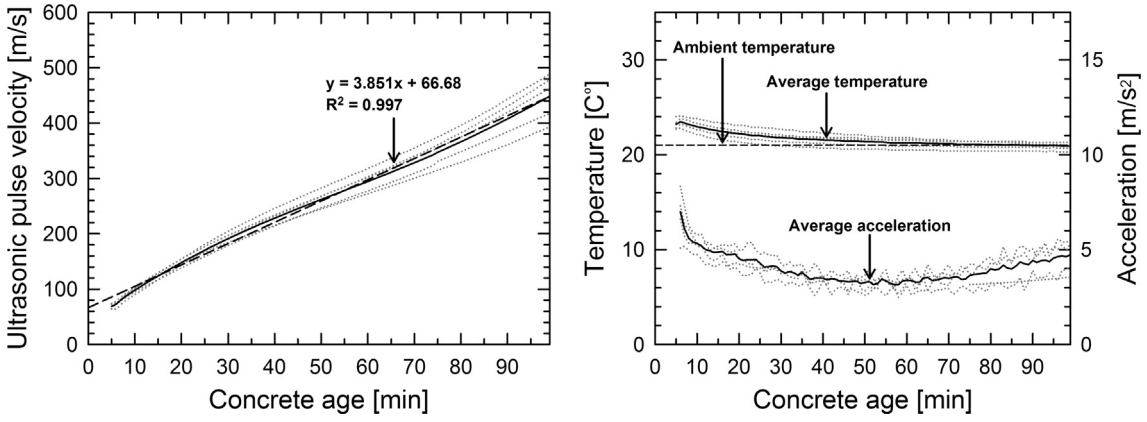

Fig. 8. Ultrasonic pulse velocity (left), and acceleration and temperature (right), measured in time using the ultrasonic wave transmission test. The grey lines indicate the individual test results, and the solid black line indicates their average. The black dashed line represents a linear fit based on the average result (left), and the ambient temperature (right).

after extrusion, was established for a specific print mortar. Both destructively determined properties were found to be linearly related to the non-destructively measured variable. As such, the ultrasonic wave transmission tests may be deemed a suitable non-destructive method to characterize the early age properties of this 3D printed mortar.

A clear transition in material failure behaviour was observed in the measured stress-strain relations of the destructive compression test at various concrete ages, and the corresponding failure modes. However, no significant increase in temperature or acceleration was measured by the ultrasonic tests during the same period, which indicates that the material is still in its dormant phase. Therefore, the gradual 'stiffening' of the material may be attributed primarily to the thixotropic build-up, rather than to setting or hardening.

For now, the findings allow continuous quality control of mechanical properties during printing on simply obtainable control batches. Furthermore, it stimulates the development of online ultrasonic monitoring methods during printing directly upon the print objects themselves.

Conflict of interest

There are no conflicts of interest to disclose.

Acknowledgements

The support of the staff of the Structures Laboratory Eindhoven is greatly acknowledged. The assistance in the 3DCP research of Master track students Structural Design at the TU/e Department of the Built Environment is highly valued. For this paper, the authors appreciate the work of R. Crombez, C. Simpelaar and M. van de Ven in particular, on whose MSc project the material presented is partially based.

The TU/e research program on 3D Concrete Printing is co-funded by a partner group of enterprises and associations, that on the date of writing consisted of (alphabetical order) Ballast Nedam, BAM Infraconsult bv, Bekaert, Concrete Valley, CRH, Cybe, Saint-Gobain Weber Beamix, SGS Intron, SKKB, Van Wijnen, Verhoeven Timmerfabriek, and Witteveen + Bos. Their support is gratefully acknowledged.

References

[1] S. Lim, R.A. Busswel, T.T. Le, S.A. Austin, A.G.F. Gibb, T. Thorpe, Developments in construction-scale additive manufacturing processes, Autom. Constr. 21 (2012) 262–268.
[2] N. Labonette, A. Rønnquist, B. Manum, P. Rüther, Additive construction: state-of-the-art, challenges and opportunities, Autom. Constr. 72 (3) (2016) 347–366.
[3] R. Duballet, O. Baverel, J. Dirrenberger, Classification of building systems for concrete 3D printing, Autom. Constr. 83 (2017) 247–258.
[4] Y.W.D. Tay, B. Panda, S.V. Paul, N.A.N. Mohamed, J.M. Tan, K.F. Leong, 3D printing trends in building and construction industry: a review, Virtual Phys. Prototyping 12 (3) (2017) 261–276.
[5] B. Khoshnevis, D. Hwang, K.T. Yao, Z. Yeh, Mega-scale fabrication by contour crafting, Int. J. Ind. Syst. Eng. 1 (3) (2006) 301–320.
[6] G. Cesaretti, E. Dini, X. de Kestelier, V. Colla, L. Pambaguian, Building components for an outpost on the Lunar soil by means of a novel 3D printing technology, Acta Astronaut. 93 (2014) 430–450.
[7] N. Hack, W.V. Lauer, F. Gramazio, M. Kohler, Mesh mould: robotically fabricated metal meshes as concrete formwork and reinforcement, in: Ferro-11 and 3rd ICTRC, Aachen, Germany, 2015.
[8] E. Lloret, A.R. Shahab, M. Linus, R.J. Flatt, F. Gramazio, M. Kohler, S. Langenberg, Complex concrete structures – merging existing casting techniques with digital fabrication, Comput. Aided Des. 60 (2015) 40–49.
[9] E. Lloret, L. Reiter, T. Wangler, F. Gramazio, M. Kohler, R.J. Flatt, Smart dynamic casting – slipforming with flexible formwork – inline measurement and control, in Second Concrete Innovation Conference (2nd CIC), Tromsø, Norway, 2017.
[10] F.P. Bos, R.J.M. Wolfs, Z.Y. Ahmed, T.A.M. Salet, Additive manufacturing of concrete in construction: potentials and challenges, Virtual Phys. Prototyping 11 (3) (2016) 209–225.
[11] C.K. Chua, C.H. Wong, W.Y. Yeong, Standards, Quality Control, and Measurement Sciences in 3D Printing and Additive Manufacturing, Academic Press, London, 2017.
[12] R.J.M. Wolfs, F.P. Bos, T.A.M. Salet, Early age mechanical behaviour of 3D printed concrete: numerical modelling and experimental testing, Cem. Concr. Res. 106 (2018) 103–116.
[13] A.S.J. Suiker, Mechanical performance of wall structures in 3D printing processes: theory, design tools and experiments, Int. J. Mech. Sci. 137 (2018) 145–170.
[14] S. Neudecker, C. Bruns, R. Gerbers, J. Heyn, F. Dietrich, K. Dröder, A. Raatz, H. Kloft, formwork, A new robotic spray technology for generative manufacturing of complex concrete structures without, Proc. CIRP 43 (2016) 333–338.
[15] R.J.M. Wolfs, F.P. Bos, E.C.F. van Strien, T.A.M. Salet, A real-time height measurement and feedback system for 3D concrete printing, in: High Tech Concrete: Where Technology and Engineering Meet, Proceedings of the 2017 fib Symposium, Maastricht, Springer, Berlin, 2017, pp. 2474–2483.
[16] N. Roussel, G. Ovarlez, S. Garrault, C. Brumaud, The origins of thixotropy of fresh cement pastes, Cem. Concr. Res. 42 (2012) 148–157.
[17] T.T. Le, S.A. Austin, S. Lim, R.A. Buswell, A.G.F. Gib, T. Thorpe, Mix design and fresh properties for high-performance printing concrete, Mater. Struct. 45 (2011) 1221–1232.
[18] A. Perrot, Y. Mélinge, D. Rangeard, F. Micaelli, P. Estellé, C. Lanos, Use of ram extruder as a combined rheo-tribometer to study the behaviour of high yield stress fluids at low strain rate, Rheol. Acta 51 (8) (2012) 743–754.
[19] V.N. Nerella, V. Mechtcherine, Virtual sliding pipe rheometer for estimating pumpability of concrete, Constr. Build. Mater. 170 (2018) 366–377.
[20] F.P. Bos, Z.Y. Ahmed, E.R. Jutinov, T.A.M. Salet, Experimental exploration of metal cable as reinforcement in 3D printed concrete, Materials 10 (11) (2017) 1–22.
[21] D.G. Soltan, V.C. Li, A self-reinforced cementitious composite for building-scale 3D printing, Cem. Concr. Compos. 90 (2018).
[22] A. Perrot, D. Rangeard, A. Pierre, Structural built-up of cement-based materials used for 3D printing extrusion techniques, Mater. Struct. 49 (4) (2015) 1213–1220.
[23] T. Wangler, E. Lloret, L. Reiter, N. Hack, F. Gramazio, M. Kohler, M. Bernhard, B. Dillenburger, J. Buchli, N. Roussel, R. Flatt, Digital concrete: opportunities and challenges, RILEM Tech. Lett. 1 (2016) 67–75.
[24] T.T. Le, S.A. Austin, S. Lim, R.A. Buswell, R. Law, A.G.F. Gibb, T. Thorpe, Hardened properties of high-performance printing concrete, Cem. Concr. Res. 42 (2012) 558–566.
[25] N. Roussel, F. Cussingh, Distinct-layer casting of SCC: the mechanical consequences of thixotropy, Cem. Concr. Res. 38 (2008) 624–632.
[26] K. Kim, S. Park, W. Kim, Y. Jeong, J. Lee, Evaluation of shear strength of RC beams with multiple interfaces formed before initial setting using 3D printing technology, Materials 10 (2017) 1–22.
[27] K. Kovler, N. Roussel, Properties of fresh and hardened concrete, Cem. Concr. Res. 41 (2011) 775–792.
[28] D. Lootens, P. Jousset, L. Martinie, N. Roussel, R.J. Flatt, Yield stress during setting of cement pastes from penetration tests, Cem. Concr. Res. 39 (2009) 401–408.
[29] Q.Y. Lu, C.H. Wong, Additive manufacturing process monitoring and control by non-destructive testing techniques: challenges and in-process monitoring, Virtual Phys. Prototyping 13 (2) (2018) 39–48.
[30] H. Yoon, Y.J. Kim, H.S. Kim, J.W. Kang, H.M. Koh, Evaluation of early-age concrete compressive strength with ultrasonic sensors, Sensors 17 (8) (2017) 1–15.
[31] H.S. Kim, Y.J. Kim, W.J. Chin, H. Yoon, Experimental study on innovative slip form method for the construction of tapered concrete pylon of long-span cable bridge, Engineering 6 (10) (2014) 633–643.
[32] T. Voigt, T. Malonn, S.P. Shah, Green and early age compressive strength of extruded cement mortar monitored with compression tests and ultrasonic techniques, Cem. Concr. Res. 36 (2006) 858–867.
[33] N. de Biele, C.U. Grosse, J. Kurz, H.W. Reinhardt, Ultrasound monitoring of the influence of different accelerating admixtures and cement types for shotcrete on setting and hardening behaviour, Cem. Concr. Res. 35 (2005) 2087–2094.
[34] R. Demirboga, I. Türkmen, M.B. Karakoc, Relationship between ultrasonic velocity and compressive strength for high-volume mineral-admixtured concrete, Cem. Concr. Res. 34 (2004) 2329–2336.
[35] L.M. del Rio, A. Jiménez, F. López, F.J. Rosa, M.M. Rufo, J.M. Paniagua, Characterization and hardening of concrete with ultrasonic testing, Ultrasonics 42 (2004) 527–530.
[36] D. Lootens, D.P. Bentz, On the relation of setting and early-age strength development to porosity and hydration in cement-based materials, Cem. Concr. Compos. 68 (2016) 9–14.
[37] H. von Daake, D. Stephan, Setting of cement with controlled superplasticizer addition monitored by ultrasonic measurements and calorimetry, Cem. Concr. Compos. 66 (2016) 24–37.
[38] G. Trtnik, M. Gams, Ultrasonic assessment of initial compressive strength gain of cement based materials, Cem. Concr. Res. 67 (2015) 148–155.
[39] Standard Test Method for Unconfined Compressive Strength of Cohesive Soil, ASTM , 2013.
[40] Testing Concrete – Part 4: Determination of Ultrasonic Pulse Velocity, European Standard EN 12504-4, 2005.

[41] J. Petit, K.H. Khayat, E. Wirquin, Coupled effect of time and temperature on variations of yield value of highly flowable mortar, Cem. Concr. Res. 36 (2006) 832–841.
[42] L.K. Mettler, F.K. Wittel, R.J. Flatt, H.J. Hermann, Evolution of strength and failure of SCC during early hydration, Cem. Concr. Res. 89 (2016) 288–296.
[43] G. Trtnik, G. Turk, F. Kavcic, V.B. Bosiljkov, Possibilities of using the ultrasonic wave transmission method to estimate initial setting time of cement paste, Cem. Concr. Res. 38 (2008) 1336–1342.
[44] W.H. Reinhardt, C.U. Grosse, Continuous monitoring of setting and hardening of mortar and concrete, Constr. Build. Mater. 18 (2004) 145–154.